Dispersion of evanescent band gap states in Fe clusters on GaAs(110)

Joseph A. Stroscio, P. N. First, R. A. Dragoset, L. J. Whitman,
D. T. Pierce, and R. J. Celotta
National Institute of Standards and Technology, Gaithersburg, Maryland 20899

(Received 10 July 1989; accepted 23 August 1989)

We report scanning tunneling microscopy results on the band gap states observed in tunneling to nanometer size metallic Fe clusters on GaAs(110) surfaces. In the vicinity of the Fe clusters, a continuum of gap states is found in tunneling spectra from regions of the bare semiconductor. The state density in the gap, emanating from the clusters, is found to decay exponentially with a decay length that is dependent on the energy in the band gap. The gap state decay length varies continuously from 3.4 Å at midgap to a divergence at the valence and conduction band edges, reflecting the characteristics of the generalized Bloch states in the semiconductor gap having complex wave vector.

I. INTRODUCTION

The relation between gap states and Schottky barrier formation has been of fundamental interest in metal-semiconductor systems since Bardeen proposed the screening properties of surface states in 1947.[1] Heine, in 1965, proposed that intrinsic surface states were not the relevant states that pin the Fermi level, since the semiconductor is covered with a metallic overlayer.[2] Heine proposed that the propagating states in the metal overlayer would decay into the semiconductor within ~ 10 Å and their charge would fix the Fermi level. These states are therefore called metal induced gap states (MIGS). Other pinning theories have been proposed that differ in the physical nature of the interface states, such as the defect model,[3] which relies on localized native defect states to be a source or sink of charge that pins the Fermi level. A basic difference between these models is that the defect model produces a set of discrete levels in the band gap, whereas the MIGS model relies on a continuum of gap states, which result from the complex band structure of the semiconductor.[4–7]

While gap states have been observed in a number of situations,[8–10] only recently has a direct correlation been made between the structural properties of the overlayer with the observation of the gap states. This was accomplished in Sb/GaAs(110) using the scanning tunneling microscope (STM).[11] In Sb/GaAs, band gap states within the Sb surface band gap were observed localized on the edges of Sb terraces.[1] In systems with metallic characteristics, the role of MIGS and the identification of the onset of metallicity has been controversial in photoelectron measurements, due to difficulty in interpreting the Fermi edge cutoff.[12] In particular, cluster formation and the onset of metallicity has been inferred from macroscopic measurements without detailed knowledge of the microscopic configurations.[13–14] The identification of single clusters and the question of metallicity has recently been investigated in the epitaxial system of Fe/GaAs(110) using the STM.[15]

In this paper, we report STM measurements of the band gap states observed in tunneling to metallic Fe clusters on GaAs(110). The observation of metallicity is apparent in the tunneling characteristics. With these metallic cluster systems, we observe a continuum of gap states throughout the GaAs band gap on regions of the bare semiconductor in the vicinity of the metallic clusters. The spatial decay of the gap states induced by the clusters is found to be dependent on the energy within the gap. Specifically, the decay length reaches a minimum of 3.4 Å at midgap and increases to a divergence at the valence and conduction band edges. These results reflect the dispersion of the complex solutions of the GaAs band structure and are very reminiscent of the MIGS states observed in theoretical calculations of metal–semiconductor interfaces.[4,5]

II. EXPERIMENTAL

The experiments were performed in an ultrahigh vacuum system with an operating pressure $<4\times10^{-11}$ Torr. Fe clusters were grown by electron beam evaporation of Fe with GaAs substrate temperatures of both 300 and 450 K. At both substrate temperatures, submonolayer Fe coverages produced three-dimensional cluster formation.[16] Fe evaporation was monitored using a quartz microbalance. Surface order and cleanliness were monitored with low-energy electron diffraction (LEED) and Auger spectroscopy before and after growth. The GaAs substrates consisted of *p*-type (Zn doped at a concentration of 2×10^{19} cm^{-3}) and *n*-type (Si doped at a concentration of 2.5×10^{18} cm^{-3}). The scanning tunneling microscope consists of a glass frame support with a double spring suspension, operating at 100 pA tunneling current. All STM images were recorded at 300 K sample temperatures. Current versus voltage (I–V) spectra were obtained at each point in the topographic images by interrupting the STM feedback loop during the I–V measurements. The tip-sample distance was decreased a fixed amount to increase the dynamic range of the I–V measurements in the region of the GaAs band gap.[17] Energies within the band gap were measured relative to the conduction band tunneling onset for *p*-type material and to the valence band edge onset for *n* type. This allowed more accurate measurements near the respective band edges, which were determined to within 0.1 eV.

III. RESULTS

Figure 1 shows a large area view of the GaAs(110) surface with deposited Fe atoms, which have formed three-di-

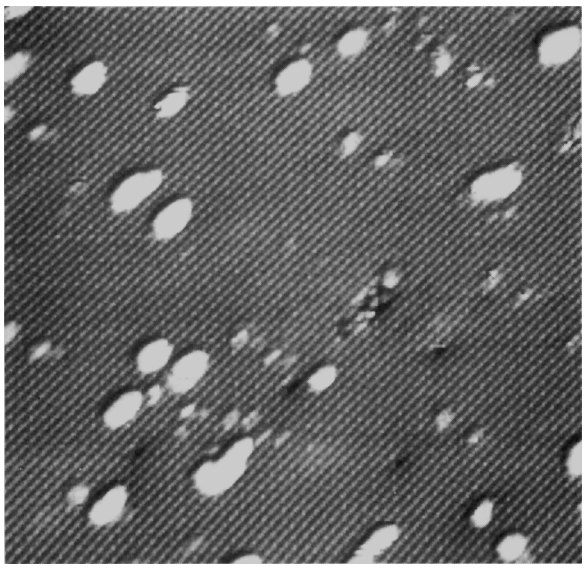

FIG. 1. STM image, 400×384 Å, of 0.1 Å Fe/*p*-GaAs(110). The sample bias was − 2.5 V. The image is displayed using a gray scale keyed to the gradient of the surface height to increase the dynamic range.

mensional clusters. The GaAs substrate appears as rows of As atoms along the [1$\bar{1}$0] direction, which is at 45° with respect to the $+x$ direction. Various size Fe clusters are observed in the image, with several different cluster heights, indicating three-dimensional cluster growth.[16] LEED observations of coalesced clusters showed the bcc Fe diffraction pattern, consistent with epitaxial growth.[18] Volume estimates of the clusters shown in Fig. 1 range from 100–1550 Å^3, corresponding to 9–127 atoms per cluster.[15]

Figure 2 shows a smaller image of two Fe clusters. The small features on the left of each cluster are satellite images due to a "double" probe tip. *I–V* characteristics were recorded at each pixel in the image using a sample and hold technique. In this way the spatial distribution of states in the band gap can be examined, since the tip position is determined by the fixed higher voltage used for imaging. Figure 3 shows a selection of the *I–V* characteristics located near the center Fe cluster, as indicated by the asterisks in Fig. 2. Curve (a) in Fig. 3 shows the Fe cluster to be metallic by the observation of a finite differential conductance, dI/dV, at zero bias. This follows since $dI/dV|_{V=0} \propto \rho(E_F)$,[19] where ρ is the surface density of states, and thus the tunneling characteristics in curve (a) indicate a partially filled band of states at the Fermi level E_F. Curves (b)–(e) still show tunneling current in the GaAs band gap, but are taken on the GaAs substrate, which usually shows no tunneling in the gap region due to a lack of states. This can be seen in curve (e), where the tunneling current in the gap region has diminished enough that the gap region can be seen. At larger distances from the cluster, a band gap of 1.5 eV is observed, which is close to the 1.4 eV gap of GaAs. The larger gap results from a small voltage drop in the semiconductor of ~0.1 eV, at 1 V applied bias.[20] The conduction band minimum is observed to be at 1.25 V, and the band bending due to the Fe clusters is measured to be 0.25 eV.

At a given voltage, the tunneling current in the gap region observed in Fig. 3 is found to decrease exponentially with distance from the Fe cluster. To show this is not due to probe tip geometry (even though probe tip effects are seen in the topograph by the appearance of satellite structures) we analyze the spatial decay of the differential conductance at energies throughout the gap. Figure 4 shows images of the differential conductance obtained from the slope of the *I–V* characteristics at two chosen voltages. Images of dI/dV in the band gap show the spatial distribution of the state density in the gap, since to first order the differential conductance is proportional to the surface density of states at an energy

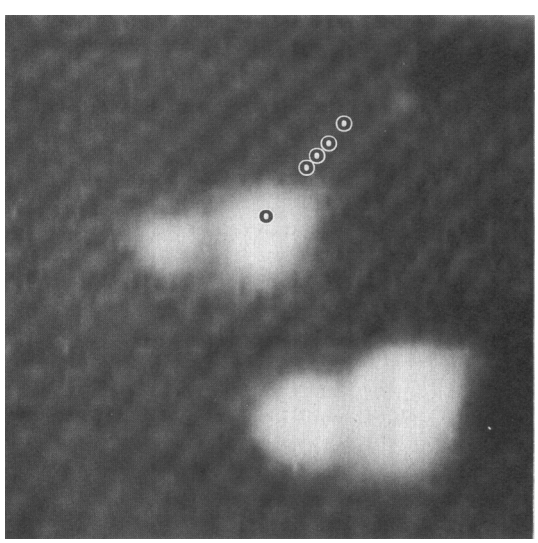

FIG. 2. STM image, 100×100 Å, of Fe clusters on *p*-GaAs(110). The sample bias was − 1.8 V. *I–V* characteristics were recorded at each pixel in the image. The circles denote the position of the *I–V* curves shown in Fig. 3.

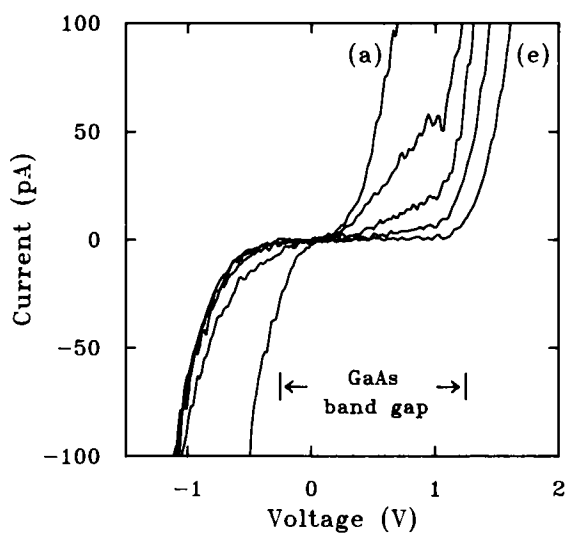

FIG. 3. Tunneling current versus distance from the Fe cluster indicated in Fig. 2. Curve (a) is on the cluster. Curves (b)–(e) correspond to distances from the cluster edge of (b) 3.7 Å, (c) 6.7 Å, (d) 9.6 Å, and (e) 14.3 Å. These tunneling characteristics were obtained with a tip-sample separation decreased by 1.0 Å relative to that used for the topograph. The valence and conduction band edges are at − 0.25 and 1.25 V, respectively.

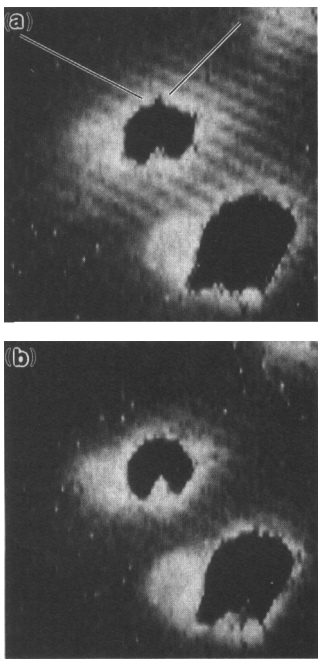

FIG. 4. Images of the logarithm of the differential conductance, $\log(dI/dV)$, obtained from the I–V characteristics recorded with the image shown in Fig. 2. The images in (a) top and (b) bottom panels correspond to voltages 1.1 and 1.0 V, respectively. (The observed conduction band minimum is at 1.25 V.) The images are shown with a gray scale ranging from 0–300 pA/V. The black regions over the clusters denote areas of large current, due to the metallic properties of the Fe clusters, which saturated our linear amplifier. The two solid lines in (a) denote the positions of the [001] and [1$\bar{1}$0] line profiles (the [1$\bar{1}$0] direction is at 45° with respect to the $+x$ direction) shown in Fig. 5.

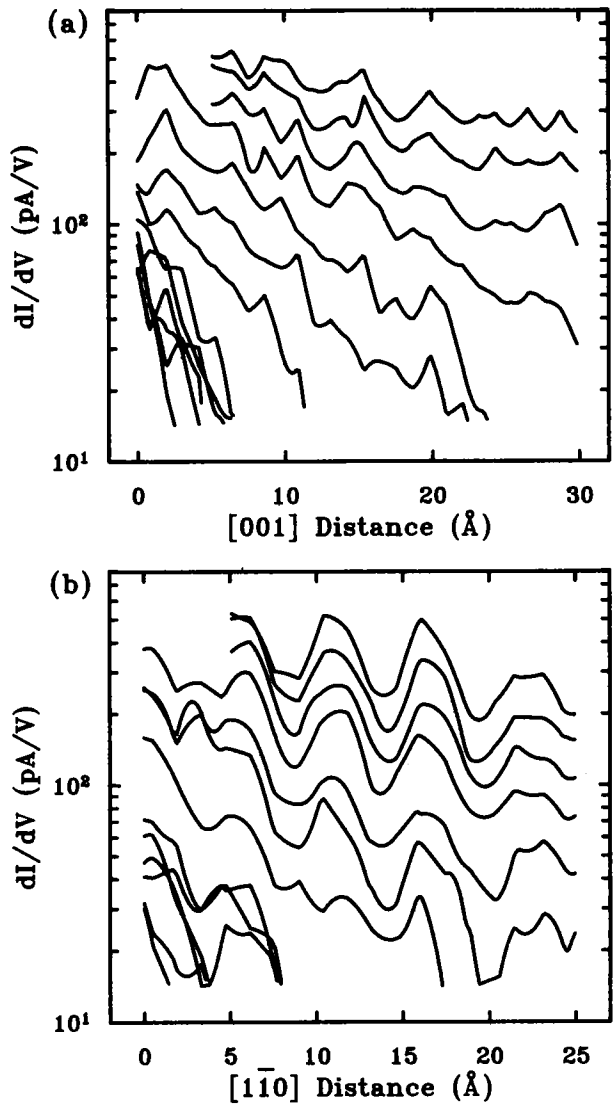

FIG. 5. Line profiles along the (a) [001] and (b) [1$\bar{1}$0] directions [indicated by the lines in Fig. 4(a)] for energies above the valence band of 0.95 to 1.55 eV in increments of 0.05 eV. The slowest decay corresponds to 1.55 eV.

E = eV with respect to the Fermi level at 0 V.[17] In Fig. 4(a), we observe a finite conductance surrounding the Fe cluster at a voltage of 1.1 V, which is 0.15 eV below the conduction band minimum. The contribution from the gap states is observed to have atomic corrugation with maxima on the Ga sites, as deduced from the phase relationship of the corrugation to that of the topograph. Figure 4(b) shows the differential conductance image at 1.0 V, just below the energy of Fig. 4(a). The region of finite conductance is found to encompass a smaller area surrounding the Fe cluster. The decay lengths observed in Figs. 4(a) and 4(b) are 16.8 and 11.4 Å, respectively, with smaller decay lengths for energies deeper in the gap.

A more quantitative examination of the decay length is made from the line profiles along the [001] and [1$\bar{1}$0] directions, as shown in Figs. 5(a) and 5(b), respectively. The energies correspond to 0.95–1.55 eV with respect to the top of the valence band, in increments of 0.05 eV. For both directions, the differential conductance (or state density) is observed to decrease exponentially with a slope that increases with energies approaching midgap. The slope of the $\log(dI/dV)$ versus distance, obtained on p-type samples from 0.7–1.6 eV, is observed to span a range of 0–0.3 Å^{-1}, with a maximum near midgap, as shown in Fig. 6(a). Results from n-type samples span the bottom portion of the gap, -0.15–0.65 eV, since the Fermi level is pinned at $\sim$0.3 eV below the conduction band minimum, for similar Fe coverages. From the n-type results, we observe a similar behavior with a maximum decay wave vector near midgap and a minimum at the valence band edge. The inverse slope, the decay length, is shown in Fig. 6(b) for energies within the band gap. The decay length is characterized by a divergence at the band edges and a minimum at midgap of 3.4 Å. From a comparison of the [001] and [1$\bar{1}$0] results, we find the decay length to be relatively isotropic in the surface plane. Data from the [1$\bar{1}$0] direction, recorded at a smaller tip-sample distance on a different Fe cluster, is also shown in Fig. 6. The decay lengths lack of dependence on tip-sample distance, as well as the observed energy dependence on both n- and p-type samples, demonstrates that the spatial decay observed in Figs. 4–6 is little influenced by the details of the probe tip geometry.[21]

IV. DISCUSSION

The existence of the gap states results from the requirement of wave function continuity across the metal–semiconductor interface. For an energy E in the gap of the semiconductor, the solutions to the Schrödinger equation will be propagating states in the metal cluster and decaying states in the semiconductor, as shown schematically in Fig. 7(a). The states in the semiconductor gap are actually generalized Bloch states of the semiconductor having complex wave vector.[2,6] The dispersion of the complex solutions from a simple

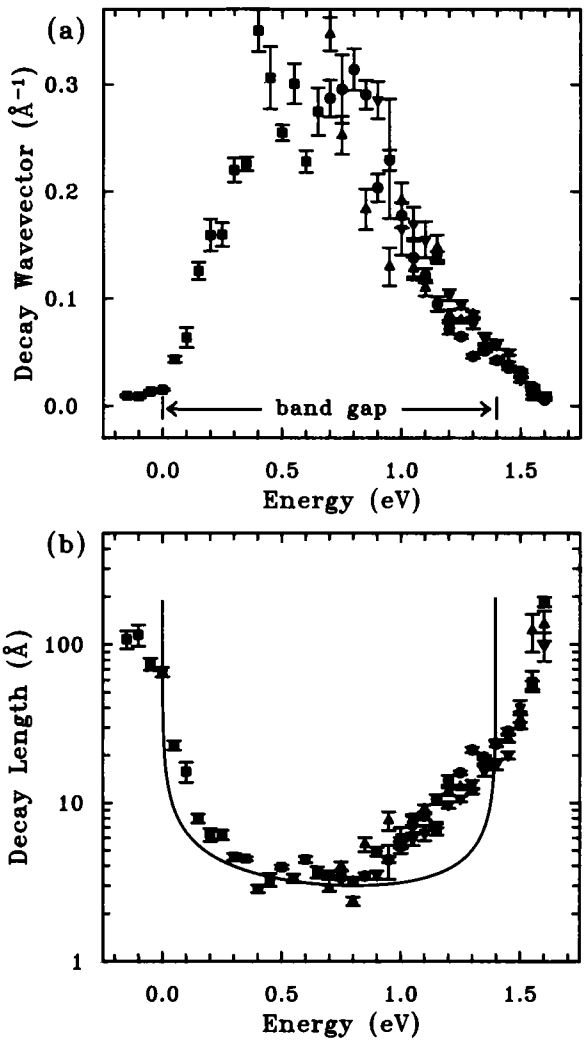

FIG. 6. Energy dependence of (a) the decay wave vector and (b) the decay length of the differential conductance obtained from the slope and inverse slope of the log (dI/dV) line profiles along the [001] (squares and circles) and [1$\bar{1}$0] (up and down triangles) directions. Data from *p*-type material is shown by the circles and triangles, and from *n* type by squares. The tip-sample separation was decreased by 1.0 (circles and up triangles from the data in Fig. 2) and 2.0 Å (squares and down triangles), relative to that used for topographic imaging. The energy scales have been shifted to give zero energy at the valence band maximum.

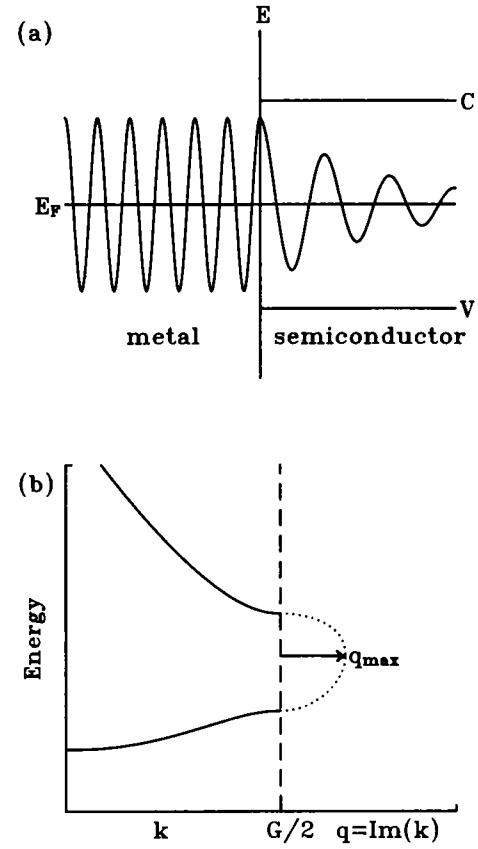

FIG. 7. (a) Schematic diagram of the energy levels at a metal-semiconductor interface and the wave function at an energy within the semiconductor band gap. (b) Energy versus wave vector for a two band model of a semiconductor. The dashed line denotes a continuation of the k axis for imaginary wave vectors at $q = 0$.

two band model is shown in Fig. 7(b).[22] In the region of the gap, the wave functions have the form $\psi(x) \propto e^{ikx} = e^{ik_r x} e^{-qx}$, where $k_r = G/2$, $q = \mathrm{Im}(k)$, and G is a reciprocal lattice vector. At the band edges, the imaginary wave vector q, goes to zero and hence the decay length diverges as the evanescent solutions go over to plane waves. Deeper in the gap, q reaches a maximum, usually near midgap between the two corresponding bands, resulting in a loop in complex reciprocal space, as shown in Fig. 7(b).[22] The experimental data shown in Fig. 6(a) reflects this complex loop.

The charge density decay length, $1/(2q)$, calculated from a two band model is shown by the solid line in Fig. 6(b). We see that it yields the qualitative features observed in the measured decay lengths, namely a divergence at the valence and conduction band edges and a minimum near midgap of 2.9 Å. This simple model yields a midgap decay length in agreement with more sophisticated calculations.[4–6] The MIGS charge density decays observed in these calculations[4,5] are very similar to the state density line profiles observed in Fig. 5. While the simple two band model shows the basic physics of gap state decay, it is a gross oversimplification and neglects the details of the three-dimensional band structure, which has multiple complex branches.[23] We also point out that the decay observed here is in the surface plane and this reduced geometry needs to be included in any theoretical model. Previous calculations have been for metal induced states decaying normal to the metal–semiconductor interface.[4,5]

V. CONCLUSION

In summary, we have shown that a continuum of gap states is observed in the vicinity of metallic nanometer size Fe clusters. These gap states emanate from the clusters and decay with a length scale that is dependent on the energy within the gap. The decay length varies from a minimum of 3.4 Å at midgap to a divergence at the valence and conduction band edges, reflecting the dispersion of the generalized Bloch states of the semiconductor having complex wave vector in the region of the band gap. Both the decay of the state density with distance and the magnitudes of the observed decay lengths are consistent with theories of metal induced gap states proposed for metal-semiconductor interfaces.

ACKNOWLEDGMENTS

We would like to thank M. Stiles, D. Penn, J. Tersoff, and R. Feenstra for stimulating discussions, and S. Mielczarek and R. Cutkosky for expert technical assistance. We gratefully acknowledge the partial support of the Office of Naval Research. P. N. First and L. J. Whitman are National Research Council Postdoctoral Research Associates.

[1]J. Bardeen, Phys. Rev. **71**, 717 (1947).
[2]V. Heine, Phys. Rev. **138**, 1689 (1965).
[3]W. E. Spicer, I. Lindau, P. R. Skeath, C. Y. Su, and P. W. Chye, Phys. Rev. Lett. **44**, 420 (1980).
[4]S. G. Louie, J. R. Chelikowsky, and M. L. Cohen, Phys. Rev. **15**, 2154 (1977).
[5]M. L. Cohen, Adv. Electronics and Elect. Phys. **51**, 1 (1980).
[6]J. Tersoff, Phys. Rev. Lett. **52**, 465 (1984).
[7]D. Troost, L. Koenders, L.-Y. Fan, and W. Monch, J. Vac. Sci. Technol. B **5**, 1119 (1987).
[8]R. Haight and J. Bokor, Phys. Rev. Lett. **56**, 2846 (1986).
[9]R. E. Viturro, M. L. Sade, and L. J. Brillson, Phys. Rev. Lett. **57**, 487 (1986).
[10]W. Drube, F. J. Himpsel, and R. Ludeke, J. Vac. Sci. Technol. B **5**, 930 (1987).
[11]R. M. Feenstra and P. Martensson, Phys. Rev. Lett. **61**, 447 (1988).
[12]W. E. Spicer and R. Cao, Phys. Rev. Lett. **62**, 605 (1989); K. Stiles and A. Kahn, *ibid.* **62**, 606 (1989); M. Prietsch, M. Domke, C. Laubschat, and G. Kaindl, *ibid.* **62**, 607 (1989).
[13]A. Zunger, Phys. Rev. B **24**, 4372 (1981).
[14]S. Doniach, K. K. Chin, I. Lindau, and W. E. Spicer, Phys. Rev. Lett. **58**, 591 (1987).
[15]P. N. First, J. A. Stroscio, R. A. Dragoset, D. T. Pierce, and R. J. Celotta Phys. Rev. Lett. **63**, 1416 (1989).
[16]R. A. Dragoset, P. N. First, J. A. Stroscio, D. T. Pierce, and R. J. Celotta, Mater. Res. Soc. Symp. Proc. **151**, 193 (1989).
[17]R. M. Feenstra, J. A. Stroscio, and A. P. Fein, Surf. Sci. **181**, 295 (1987).
[18]G. A. Prinz and J. J. Krebs, Appl. Phys. Lett. **39**, 397 (1981).
[19]J. Tersoff and D. R. Hamann, Phys. Rev. Lett. **50**, 1998 (1983); Phys. Rev. B **31**, 805 (1985).
[20]R. M. Feenstra and J. A. Stroscio, J. Vac. Sci. Technol. B **5**, 923 (1987).
[21]A probe tip effect (i.e., double imaging), is observed in the topographic image of the Fe cluster due to the large vertical asperity of the cluster. It is not seen on the relatively flat substrate as evidenced from the observed atomic corrugation in Fig. 2. However, the effect of the "double" tip does obscure the gap state decay in the region of the satellite image of the cluster, as would be expected.
[22]See for example, C. Kittel, *Introduction to Solid State Physics* (Wiley, New York, 1976), p. 199.
[23]D. L. Smith and C. Mailhiot, Phys. Rev. B **33**, 8345 (1986).